

A hybrid robot for robot-assisted orthopaedic surgery

*S.J. Yan¹⁾, S.K. Ong²⁾ and A.Y.C. Nee³⁾

^{1), 2), 3)} *Department of Mechanical Engineering,
National University of Singapore, Singapore*
¹⁾ shijuny@nus.edu.sg

ABSTRACT

Recent research on surgical robotics shows that higher accuracy can be achieved with robot-assisted than manual surgical operations. Most of the surgical robots belong to the serial architecture which has a large workspace but lower accuracy and payload-to-weight ratio, while parallel manipulators present high accuracy and payload-to-weight ratio but a limited workspace. Combining the advantages of these two different mechanisms, a hybrid robot, which consists of a serial robot and a parallel manipulator, is proposed to assist surgeons in orthopaedic surgery. Aiming to identify the assembly errors of the hybrid robot and simultaneously simplify the registration of the hybrid robot in the preoperative stage, a stereo camera is proposed to calibrate the hybrid robot using the product of exponentials (POE) method. This calibration helps to identify the transformation between the serial robot and the parallel manipulator, and the transformation between the serial robot's base and a global coordinate frame.

1. INTRODUCTION

Robot-assisted surgery is a vibrant research topic as it brings good benefits to medical care. This medical application aims at using robots to help surgeons perform accurate and delicate surgical operations. Currently, surgical robotics is leading a revolution in the development of surgical devices, operation procedures and philosophy.

With the potential advantages of applications of serial robots in medical care, several robotic systems have come into clinical use for orthopaedic surgery. ROBODOC is one of the robotic systems for orthopaedic surgery, which was developed for precise bone machining in total hip replacement in 1990s (Taylor 1994). The ROBODOC system is always classified into a category of active surgical systems, since the robot can exercise active operations on patients without direct interaction with surgeons while in operation. It has been cleared by the FDA, and has been used in over 24,000 combined TKA and THA surgeries worldwide, according to Curexo Technology Corporation. Different from ROBODOC, Acrobot is probably one of the most famous passive surgical systems, which was developed at Imperial College (Jakopec 2001). The technique of active constraint control makes Acrobot's motion

¹⁾ Graduate student

²⁾ Associate professor

³⁾ Professor

constrained in predefined regions. With this technique, the system can provide stability to eliminate the unsteadiness of surgeons' hands. Similar with Acrobot, MAKO Tactile Guidance System (TGS) belongs to the category of passive surgical systems (Tarwala 2011), which has gained regulatory approval.

As can be seen, most of the clinically-used or under-development surgical robots are based on serial mechanisms (Baena 2010), since the serial mechanisms can produce a large work volume and have high dexterity. However, both low applied force capacity and low payload-to-weight ratio limit the applications of serial robots and cause these mechanisms. To achieve high accuracy, parts of high stiffness and high accuracy have to be used to build these robots, which might make these robots become costly. Compared with the serial mechanisms, parallel mechanisms, generally possess high rigidity, high payload-to-weight ratio and are capable of achieving high accuracy at low cost.

The development of surgical robots using parallel architecture is also underway (Kratchman 2011, Nakano 2009, Tang 2012, Tian 2010). Brandt (1999) used a compact parallel robot known as Stewart Platform (SP) in orthopaedic surgery. The system was known as CRIGOS and accuracy tests yielded promising results. However, parallel mechanisms suffer from small work volume and low dexterity. To overcome these problems, Shoham (2003) proposed a bone-mounted miniature parallel robot for spine surgery. This miniature robot, known as MARS, was directly mounted on the patient's vertebra near the surgical site. With tests on animals, the deviation was claimed to be less than 1mm due to forces and moments acting on the robot by the surgeon.

Nevertheless, the method of attaching a robot on the patient's bone makes it difficult to achieve minimal invasive surgery, since the robot's fixation can cause damages on the patients' tissues during operation. As stated above, serial mechanisms have greater flexibility and larger workspace but lower payload-weight ratio and accumulative inaccuracy, while parallel mechanisms have limited workspace but higher payload-weight ratio and higher accuracy. A hybrid robot, which consists of a serial robot and a parallel manipulator, combines the advantages of these two different mechanisms. Evolution 1 precision robot, which is a hybrid robot, was investigated by Zimmermann (2004) in neuro-endoscopic procedures. After several experiments on three patients, the actual operation time was found to be comparable with manual operations, and the precision was noteworthy. Thus, this paper proposes a hybrid robot for orthopaedic surgery. To guarantee the accuracy of the hybrid robot, a calibration method with a stereo camera is also proposed to make the calibration more convenient.

This paper is organized as follows. After a description of the structure of the hybrid robot, its operating mode is discussed in section 3. The calibration method is presented in section 4 with identified parameters and solving algorithm, followed by the calibration results in section 5. Finally, a brief conclusion is given with some discussions and future works.

2. STRUCTURE OF THE HYBRID ROBOT

The hybrid robot comprises of a serial robot and a parallel manipulator, which is illustrated in Fig. 1. The serial robot is a five-axis industrial robot SCORBOT. Its main

function is to provide high dexterity of locating the parallel manipulator. In the preoperative stage, the spatial location of the parallel manipulator is obtained based on the positions of patients' anatomies and planned operations. After the motion planning stage, the serial robot works as a rough positioner to position the parallel manipulator. The position of the end effector of the parallel manipulator is tracked using a stereo camera. The positioning error caused by the serial robot can be compensated by the motion of the parallel manipulator. The parallel manipulator, known as a triglide, has three degrees of freedom (DOF) and is purely translational (Fig. 2). The triglide consists

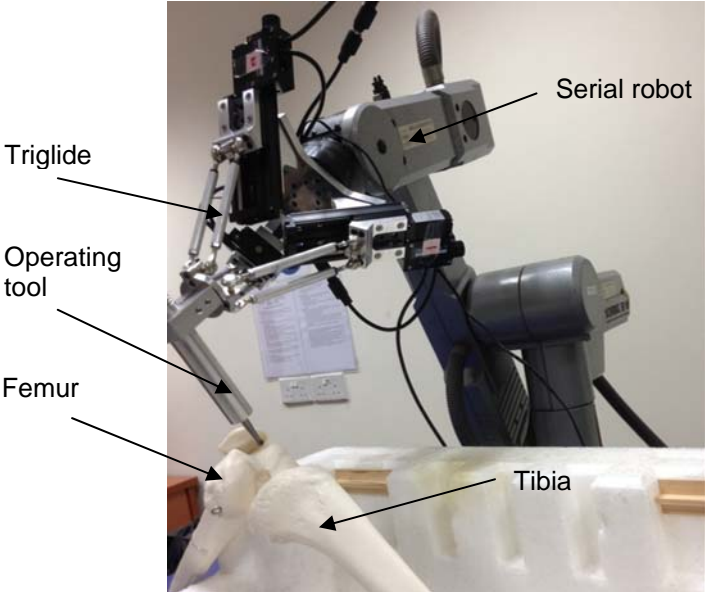


Fig. 1 Configuration of a hybrid robot

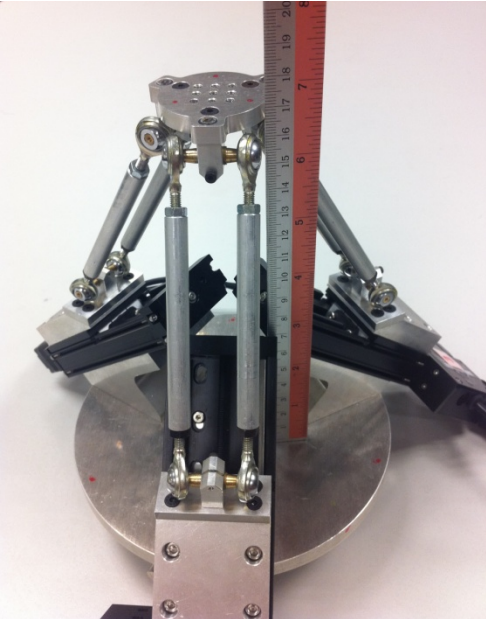


Fig. 2 Structure of the triglide

of a base plate, a mobile platform and three identical parallelogram limbs which connect the mobile platform with the base plate. Three prismatic actuators are distributed symmetrically on the base plate. The parallelogram structures constrain the orientation motion of its mobile platform, so that the mobile platform can achieve only pure translations. In the intraoperative stage, the actuators drive the mobile platform to machine patients' bones with operation tools.

3. ACTIVE OR PASSIVE

Most of robotic systems applied in surgeries fall into three categories, namely, tele-surgical system, passive surgical system and active surgical system. A tele-surgical system is also known as a remote-surgery system, with which surgeons operate at a console, monitor the whole process through a display screen, and perceive force feedback through a sensory system. A passive robotic system is not absolutely passive. It is also classified as semi-active or shared control system. It works as an assistant to surgeons and provides active constraints to the motions of the surgeons' hands. With this system, the surgeons would have to operate surgical instruments directly, and hence the system is called as a hand-on robot by some researchers (Jakopec 2003). These two systems are also called assistive/collaborative devices by Gomes (2011). The most automated system of these three categories is the active system. Robots in this system can exercise autonomous operations on patients. Although the robots can take over many operations, surgeons are still needed to undertake preparations which might be more than the other two systems. Usually, the preparations include registrations of patients' anatomies and the robots, and motion planning of the robots.

For orthopaedic surgery, robotic systems usually adopt the active/passive approach, such as ROBODOC, which is an example of the active system, and MAKO TGS, which belongs to a passive system. Few studies present a thorough comparison between active and passive robotic systems for orthopaedic surgery. Since the end effector of a passive robotic system is operated directly by a surgeon's hands, the operated bone surface is difficult to be as accurate as that operated by an active robotic system. However, it is essential for the surgeon to be present during the whole operation. With a passive system, it also makes the patients feel reassured if the robot only works as an assistive tool, and the surgeon is dominant in completing the operation. Compared with passive systems, active systems may achieve higher accuracy since the robots actively carry out the operations on the subject. Unfortunately, there are few follow-up reports about patients operated by robotic systems, which can prove that higher operation accuracy achieved with robotic systems is able to benefit patients if only considering their long-term health reports. Additionally, active robotic systems cannot be as intelligent or experienced as surgeons. Their active operation may cause serious damage in practice, since motion planning can only be done in virtual environment. For safety consideration, the active robots should be intelligent and equipped with sufficient information to help them make an optimal decision if the physical environment is changed or an unpredicted situation is encountered.

To overcome the difficulties of risk management, the hybrid robot proposed in this paper can work as a tele-surgical system. Two handles will be designed for surgeons to

control the hybrid robot, so that the hybrid robot can mimic the motions of the surgeons' hands. On the other hand, the hybrid robot can be set to move actively if it is working in a low-risk situation, such as the operating tool is still far away from vulnerable tissues or far away from areas which are forbidden to access in operations, while the surgeon can take over the control through the handles at any time. In this case, this system is neither a completely active system nor a completely tele-surgical system.

4. CALIBRATION

The triglide is designed to be fixed on the end effector of the serial robot in the preoperative stage. During idle time, this fixation increases the load of the serial robot. Additionally, an operating room should not be too crowded. For this reason, an equipment which can be applied in several operations can save space in the operating room. Hence, detachment of the triglide from the serial robot allows the serial robot to be used in other applications. In this case, the triglide is attached on the serial robot before an operation, and detached after the operation. The attachment and detachment can become routine procedures. Therefore, any assembly error caused by the attachment should be calibrated each time when the triglide is fixed before the operation.

Since the calibration becomes a routine procedure, a simple and efficient method is needed to make the calibration more convenient and shorten the calibration time. Considering that the position of the operation tool has to be intraoperatively tracked by a tracking system, many researchers (Bootsma 2008; Mozes 2010) have adopted stereo cameras as the main tracking equipment. A stereo camera is proposed to calibrate the hybrid robot, so that this stereo camera can also be used for in the subsequent tracking process in the intraoperative stage. For the calibration of a serial robot, autonomous visual measurement has been proposed by several researchers (Meng 2007; Watanabe 2006). In their method, a single camera is installed on the end effector of the serial robot. After moving the robot to several different configurations, the camera and the robot can be calibrated simultaneously. Compared with the method with a single camera, the stereo camera is able to measure the spatial pose of an object. It is unnecessary to fix the camera on the robot, and hence the camera can stand on the ground with the same configuration of the subsequent tracking process.

4.1 Identification of calibration parameters

As stated above, the parameters which will be identified should contain the transformation of the local coordinate frame of the triglide relative to the local coordinate frame attached with the end effector of the serial robot. This transformation can be denoted as T_b .

Besides T_b , the transformation of the base coordinate frame of the serial robot relative to a global coordinate frame should also be identified. This is necessary as the hybrid robot and a patient's anatomy should be registered on a global coordinate frame, so that the hybrid robot is able to know the accurate location of the patient's anatomy.

This transformation is represented by T_a . Since the same stereo camera is used for registration, the reference coordinate frame of the camera is defined as the global frame. The calibration scheme and identified parameters are depicted in Fig. 3. In this figure, O_i denotes the origin of coordinate frame i , and j_iT is the transformation of coordinate frame j relative to i . The transformation 4_0T is obtained by pose measurement of the mobile platform of the triglide with the stereo camera. The transformations 2_1T and 4_3T are respectively retrieved from the kinematics of the serial robot and the triglide.

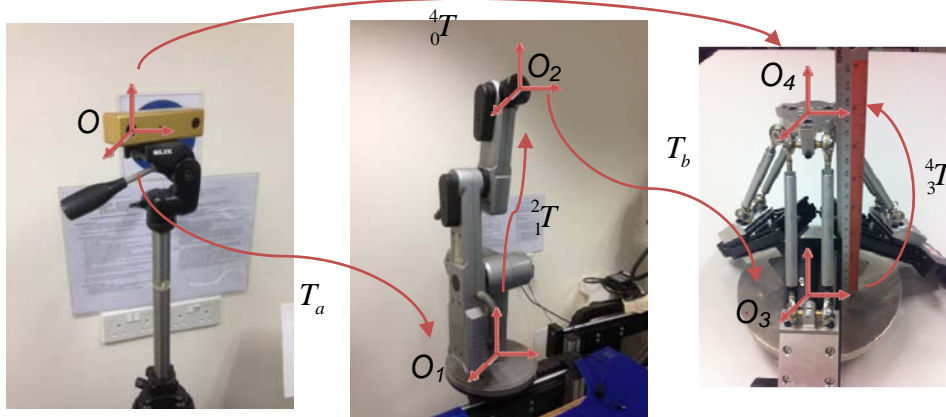


Fig. 3 Calibration scheme of the hybrid robot

4.2 Pose measurement

To reduce the effects of measurement errors, a chessboard-pattern sheet is pasted on the mobile platform of the triglide. The stereo camera is used to obtain the coordinates of all the inner points where adjacent black squares intersect with each other in the chessboard (figure 4). Supposing that X_i denotes the coordinate of each point in the sheet and Y_i denotes the coordinate obtained by the camera

$${}^4_0TX_i = Y_i, \quad (1)$$

Caused by measurement errors, it is impossible to find one transformation matrix 4_0T to make equation (1) hold with all the measurement data. The pattern sheet provides redundant information. Hence, an optimal 4_0T can be obtained to minimize Eq. (2).

$$\sum \left\| {}^4_0TX_i - Y_i \right\|, \quad (2)$$

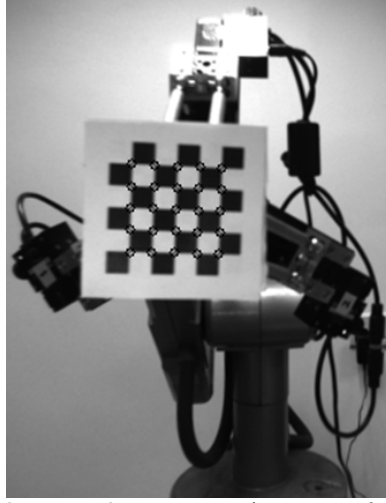


Fig. 4 Identified intersecting corners (centers of the black circles)

The Coherent Point Drift (CPD) method (Myronenko 2010) is used to solve this optimal 4_0T . The CPD method aligns X_i with Y_i , considering that the point sets of X_i are represented by Gaussian Mixture Model (GMM) centroids. The alignment problem is to maximize the likelihood of fitting the centroids to Y_i .

4.3 Calibration method

The Product of Exponentials (POE) formula is used to solve the calibration problem. According to Okamura (1996), the POE method can avoid kinematic singularity problems which always happen in the kinematic representations based on the Denavit-Hartenberg parameters. With the POE method, each rigid transformation is represented by $e^{\hat{\xi}_i}$. $\hat{\xi}_i$ denotes the twist of the i th joint, which belongs to the Lie algebra $se(3)$ of the special Euclidean group $SE(3)$. If v_i denotes the position vector of the i th joint axis, and $\hat{\omega}_i$ denotes the skew-symmetric matrix of ω_i , which is the unit directional vector of the i th joint axis, equation (3) can be obtained,

$$\hat{\xi}_i = \begin{bmatrix} \hat{\omega}_i & v_i \\ 0 & 0 \end{bmatrix}, \quad (3)$$

where $\omega_i = [\omega_{1i} \ \omega_{2i} \ \omega_{3i}]^T$, $v_i = [v_{1i} \ v_{2i} \ v_{3i}]^T$, and

$$\xi_i = \begin{bmatrix} v_i \\ \omega_i \end{bmatrix}, \quad \hat{\omega}_i = \begin{bmatrix} 0 & -\omega_{3i} & \omega_{2i} \\ \omega_{3i} & 0 & -\omega_{1i} \\ -\omega_{2i} & \omega_{1i} & 0 \end{bmatrix}.$$

For the hybrid robot, its forward kinematics can be represented as

$$f = e^{\hat{\xi}_1} e^{\hat{p}_1} e^{\hat{\xi}_2} e^{\hat{p}_2}, \quad (4)$$

where $e^{\hat{\xi}_1} = T_a$, $e^{\hat{p}_1} = {}^2T$, $e^{\hat{\xi}_2} = T_b$, $e^{\hat{p}_2} = {}^4T$.

The calibration can identify T_a and T_b . Only the errors in $e^{\hat{\xi}_1}$ and $e^{\hat{\xi}_2}$ are considered. The error model can be obtained as

$$df = d(e^{\hat{\xi}_1})e^{\hat{p}_1}e^{\hat{\xi}_2}e^{\hat{p}_2} + e^{\hat{\xi}_1}e^{\hat{p}_1}d(e^{\hat{\xi}_2})e^{\hat{p}_2}, \quad (5)$$

If right multiplied by f^{-1} , Eq. (6) can be obtained.

$$df \cdot f^{-1} = d(e^{\hat{\xi}_1}) \cdot e^{-\hat{\xi}_1} + e^{\hat{\xi}_1}e^{\hat{p}_1}d(e^{\hat{\xi}_2}) \cdot e^{-\hat{\xi}_2}e^{-\hat{p}_1}e^{-\hat{\xi}_1}, \quad (6)$$

The identification problem becomes solving the cost function in Eq. (7).

$$\text{Min} \sum \left\| df \cdot f^{-1} - A_1 d\xi_1 - Ad_{e^{\hat{p}_1}e^{\hat{\xi}_1}} A_2 d\xi_2 \right\|^2, \quad (7)$$

With the explicit expression given in (Ruibo 2010), Eq. (8) can be obtained.

$$\left[df \cdot f^{-1} \right]^\vee = A_1 d\xi_1 + Ad(e^{\hat{\xi}_1}e^{\hat{p}_1})A_2 d\xi_2 \quad (8)$$

where $Ad(X)$ is the adjoint transformation, and

$$A_i = I_6 + \frac{4 - \|\omega_i\| \sin \|\omega_i\| - 4 \cos \|\omega_i\|}{2 \|\omega_i\|^2} \Omega_i + \frac{4 \|\omega_i\| - 5 \sin \|\omega_i\| + \|\omega_i\| \cos \|\omega_i\|}{2 \|\omega_i\|^3} \Omega_i^2 \\ + \frac{2 - \|\omega_i\| \sin \|\omega_i\| - 2 \cos \|\omega_i\|}{2 \|\omega_i\|^4} \Omega_i^3 + \frac{2 \|\omega_i\| - 3 \sin \|\omega_i\| + \|\omega_i\| \cos \|\omega_i\|}{2 \|\omega_i\|^5} \Omega_i^4,$$

and

$$\Omega_i = \begin{bmatrix} \hat{\omega}_i & 0 \\ \hat{v}_i & \hat{\omega}_i \end{bmatrix}.$$

If letting $Y = \left[df \cdot f^{-1} \right]^\vee$, $J = \left[A_1 \quad Ad(e^{\hat{\xi}_1}e^{\hat{p}_1})A_2 \right]$, and $X = \left[d\xi_1 \quad d\xi_2 \right]^T$, Eq. (8) can be expressed as

$$Y = JX \quad (9)$$

If letting T_c and T_m be the computed and measured values of 4T , equation (10) can be obtained.

$$df \cdot f^{-1} = \log(T_m \cdot T_c^{-1}) \quad (10)$$

An iterative Levenberg-Marquardt method can be used to solve the cost function. The solving process is illustrated in Fig. 5.

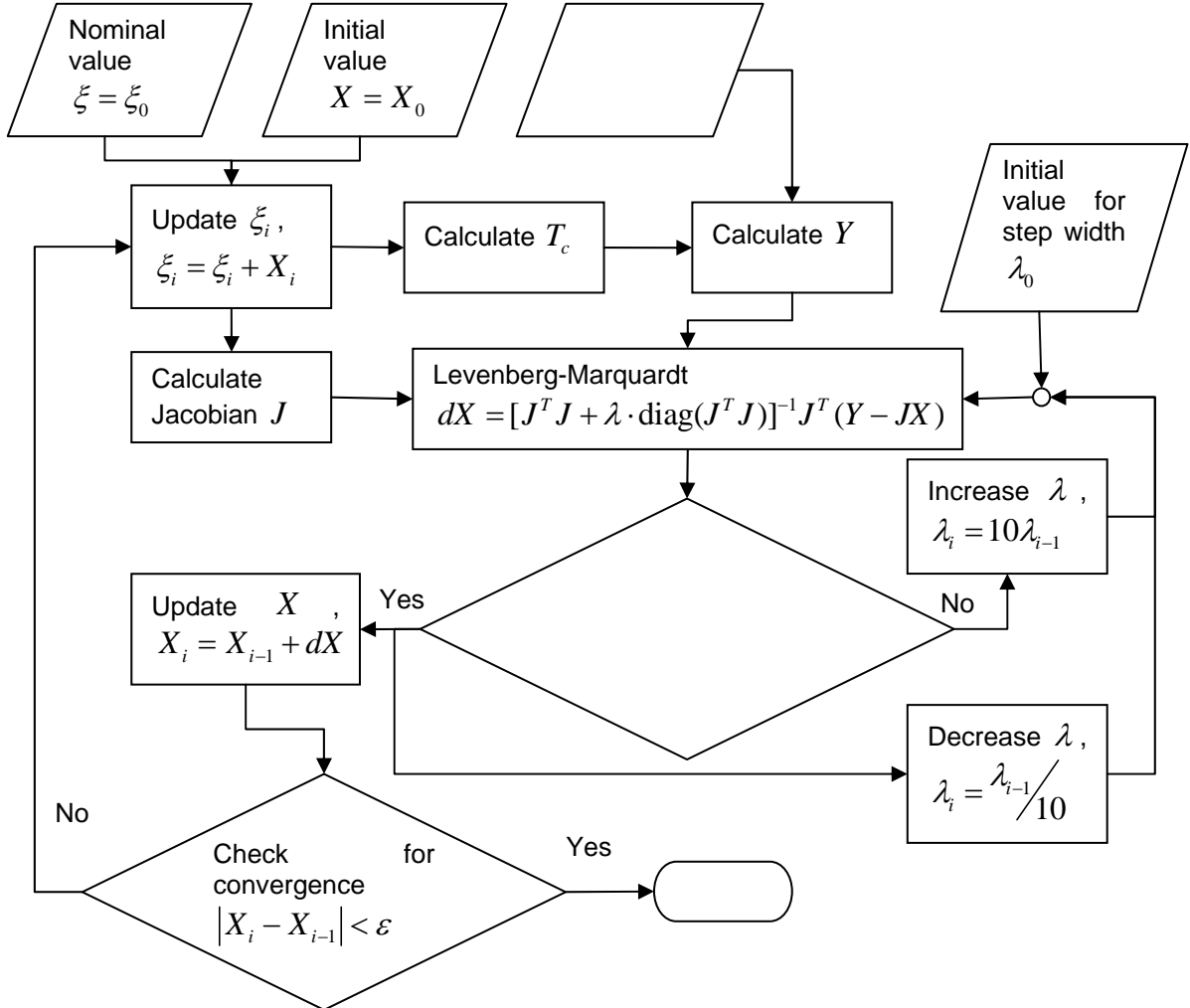


Fig. 1 Flow chart of parameter identification with Levenberg-Marquardt method

5. RESULTS

This section presents the calibration results. The position and orientation errors of the hybrid robot after calibration are also presented in this section.

This calibration contains 12 parameters which need to be identified. The error model for each measurement provides an equation system including six equations. Therefore, two measurements can be used to solve the 12 parameters theoretically. Since more measurements can decrease the effects of measurement errors, the number of measured poses is set to 30.

The nominal values of these parameters, which are also their initial values, are listed in Table 1, as well as their identified results. As stated above, $e^{\hat{\xi}_1}$ and $e^{\hat{\xi}_2}$ equal to the transformations of T_a and T_b respectively. The nominal value of ξ_1 is estimated, since it is difficult to obtain the position and orientation of the local coordinate frame of the serial robot with respect to the global coordinate.

To clearly interpret the position error and orientation error of the hybrid robot after calibration, the computed pose and measured pose of the mobile platform of the triglide are respectively denoted by $e^{\hat{\xi}_c}$ and $e^{\hat{\xi}_m}$, where $\xi_c = [v_c \ \omega_c]^T$ and $\xi_m = [v_m \ \omega_m]^T$. The relationship between $\hat{\xi}_i$ and ξ is shown in Eq. (3). The position error is defined as

Table 1 Nominal and identified values of the unknown parameters in the calibration

	Nominal values	Identified results
ξ_1	$[0 \ 0 \ 600 \ 0 \ 0 \ 0]^T$	$[22.004 \ 19.846 \ 750.650 \ 0.002 \ -0.002 \ 0]^T$
ξ_2	$[0 \ 0 \ 10 \ 0 \ 0 \ 0]^T$	$[1.693 \ -0.063 \ 9.529 \ 0 \ 0.001 \ 0.001]^T$

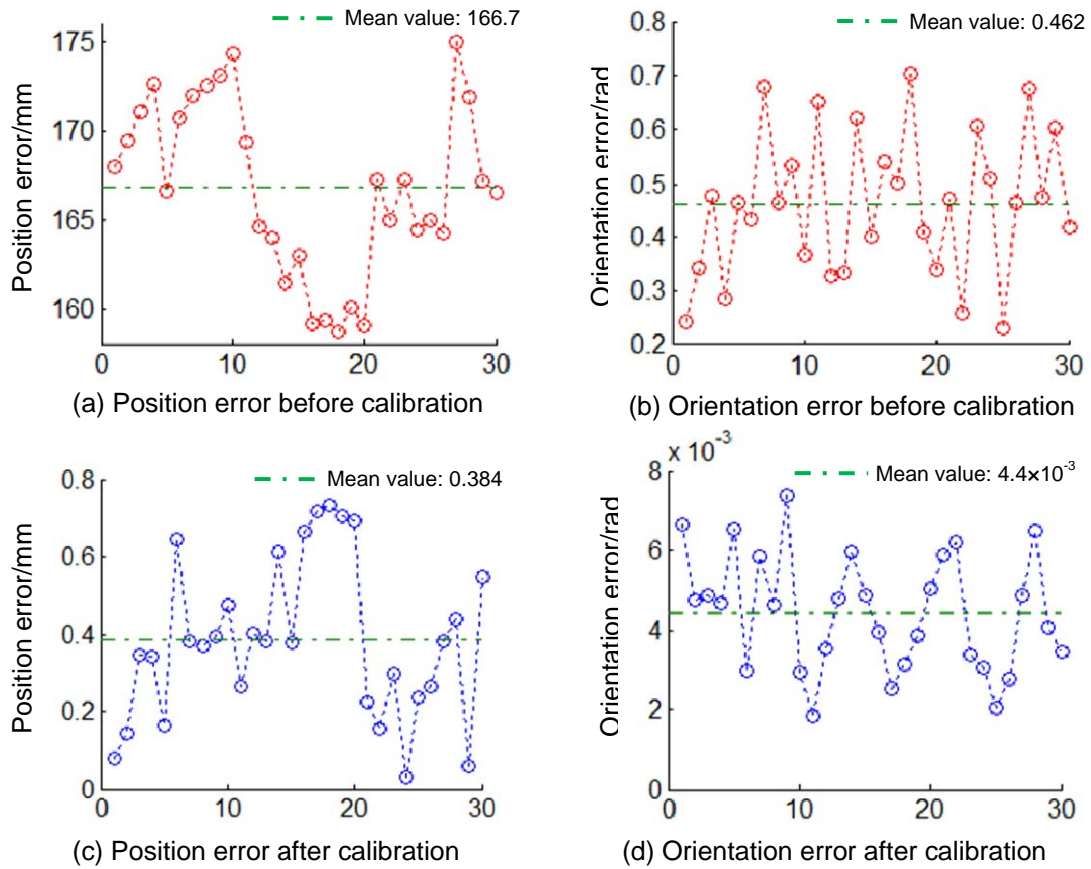


Fig. 6 Differences between measured poses and computed poses of the hybrid robot before and after calibration

$$e_p = \|v_c - v_m\|_2, \quad (11)$$

and the orientation error is obtained as

$$e_r = \|\omega_c - \omega_m\|_2, \quad (12)$$

Fig. 6 also illustrates the position and orientation errors of the hybrid robot before calibration.

From Fig. 6, it can be seen that the position and orientation errors before calibration are very large. These large errors are mostly caused by the estimated T_a . Since the stereo camera is placed arbitrarily, it is difficult to obtain an accurate T_a without calibration. After calibration, the errors decrease significantly. The largest position error is less than 0.8mm after calibration and the mean value of the position errors is 0.384mm, which is comparable with the accuracy obtained in (Meng 2007) using vision technology. After calibration, the orientation of the hybrid robot is more accurate, since the largest orientation error is less than 8×10^{-3} rad and the mean value is only 4.4×10^{-3} rad.

6. CONCLUSIONS

A hybrid robot is proposed in this paper for orthopaedic surgery. The hybrid robot uses a five-axis serial robot for rough positioning and a three-DOF purely translational parallel manipulator for fine tuning. As the widespread concern of active surgical systems and limited accuracy of passive surgical systems, the hybrid robot can move actively, and also can work as a tele-surgical system. Whether it works actively or passively can be decided according to the risk level of working environment and surgeon's experience.

For convenient identification of the transformation between the parallel manipulator and the serial robot and the registration of the serial robot on to a global coordinate system, a calibration method is proposed using a stereo camera to identify the pose of the end effector of the hybrid robot. The calibration is implemented with the POE method. After calibration, the position accuracy and orientation accuracy can be improved significantly. The error is also comparable with other researchers' results obtained with vision technology.

Although the accuracy can be greatly improved, this calibration method is not compared with other methods, such as measurement with a laser scanner used in (Ernst 2012). Thus, a comparison with other calibration methods will be carried out in future work.

REFERENCES

Baena, F.R.y and Davies, B. (2010), "Robotic surgery: from autonomous systems to intelligent tools", *Robotica*, (28), 163-170. DOI: 10.1017/S0263574709990427

- Bootsma, G.J., Siewerdsen, J.H., Daly, M.J. and Jaffray, D.A. (2008), "Initial investigation of an automatic registration algorithm for surgical navigation", *Engineering in Medicine and Biology Society, EMBS 2008, 30th Annual International Conference of the IEEE*. DOI: 10.1109/IEMBS.2008.4649996
- Brandt, G., Zimolong, A., Carrat, L., Merloz, P., Staudte, H.W., Lavallee, S., Radermacher, K., *et al.* (1999), "CRIGOS: a compact robot for image-guided orthopedic surgery", *Information Technology in Biomedicine, IEEE Transactions on*, **3**(4), 252-260.
- Ernst, F., Richter, L., Matthäus, L., Martens, V., Bruder, R., Schlaefer, A. and Schweikard, A. (2012), "Non-orthogonal tool/flange and robot/world calibration", *The International Journal of Medical Robotics and Computer Assisted Surgery*, **8**(4), 407-420. DOI: 10.1002/rcs.1427
- Gomes, P. (2011), "Surgical robotics: Reviewing the past, analysing the present, imagining the future", *Robotics and Computer-Integrated Manufacturing*, **27**(2), 261-266. DOI: 10.1016/j.rcim.2010.06.009
- Jakopec, M., Harris, S.J., Rodriguez y Baena, F., Gomes, P., Cobb, J. and Davies, B.L. (2001), "The First Clinical Application of a "Hands-On" Robotic Knee Surgery System", *Computer Aided Surgery*, **6**(6), 329-339. DOI: 10.3109/10929080109146302
- Jakopec, M., Rodriguez y Baena, F., Harris, S.J., Gomes, P., Cobb, J. and Davies, B.L. (2003), "The hands-on orthopaedic robot "acrobot": Early clinical trials of total knee replacement surgery", *Robotics and Automation, IEEE Transactions on*, **19**(5), 902-911. DOI: 10.1109/tra.2003.817510
- Kratchman, L.B., Blachon, G.S., Withrow, T.J., Balachandran, R., Labadie, R.F. and Webster, R.J. (2011), "Design of a Bone-Attached Parallel Robot for Percutaneous Cochlear Implantation", *Biomedical Engineering, IEEE Transactions on*, **58**(10), 2904-2910. DOI: 10.1109/tbme.2011.2162512
- Meng, Y. and Zhuang, H. (2007), "Autonomous robot calibration using vision technology", *Robotics and Computer-Integrated Manufacturing*, **23**(4), 436-446. DOI: <http://dx.DOI.org/10.1016/j.rcim.2006.05.002>
- Mozes, A., Chang, T.-C., Arata, L. and Zhao, W. (2010), "Three-dimensional A-mode ultrasound calibration and registration for robotic orthopaedic knee surgery", *The International Journal of Medical Robotics and Computer Assisted Surgery*, **6**(1), 91-101. DOI: 10.1002/rcs.294
- Myronenko, A. and Song, X. (2010), "Point Set Registration: Coherent Point Drift", *Pattern Analysis and Machine Intelligence, IEEE Transactions on*. DOI: 10.1109/TPAMI.2010.46
- Nakano, T., Sugita, N., Ueta, T., Tamaki, Y. and Mitsuishi, M. (2009), "A parallel robot to assist vitreoretinal surgery", *International Journal of Computer Assisted Radiology and Surgery*, **4**(6), 517-526. DOI: 10.1007/s11548-009-0374-2
- Okamura, K. and Park, F.C. (1996), "Kinematic calibration using the product of exponentials formula", *Robotica*, **14**(04), 415-421. DOI: 10.1017/S0263574700019810
- Ruibo, H., Yingjun, Z., Shunian, Y. and Shuzi, Y. (2010), "Kinematic-Parameter Identification for Serial-Robot Calibration Based on POE Formula", *Robotics, IEEE Transactions on*, **26**(3), 411-423. DOI: 10.1109/tro.2010.2047529

- Shoham, M., Burman, M., Zehavi, E., Joskowicz, L., Batkilin, E. and Kunicher, Y. (2003), "Bone-mounted miniature robot for surgical procedures: Concept and clinical applications", *Robotics and Automation, IEEE Transactions on*, **19**(5), 893-901.
- Tang, P., Hu, L., Du, H., Gong, M. and Zhang, L. (2012), "Novel 3D hexapod computer-assisted orthopaedic surgery system for closed diaphyseal fracture reduction", *The International Journal of Medical Robotics and Computer Assisted Surgery*, **8**(1), 17-24. DOI: 10.1002/rcs.417
- Tarwala, R. and Dorr, L. (2011), "Robotic assisted total hip arthroplasty using the MAKO platform", *Current Reviews in Musculoskeletal Medicine*, **4**(3), 151-156. DOI: 10.1007/s12178-011-9086-7
- Taylor, R.H., Mittelstadt, B., Paul, H.A., Hanson, W., Kazanzides, P., Zuhars, J.F., Williamson, B., *et al.* (1994), "An image-directed robotic system for precise orthopaedic surgery", *Robotics and Automation, IEEE Transactions on*, **10**(3), 261-275. DOI: 10.1109/70.294202
- Tian, H.Q., Wu, D.M., Du, Z.J. and Sun, L.N. (2010), "Design and analysis of a 6-DOF parallel robot used in artificial cervical disc replacement surgery", *Information and Automation (ICIA), 2010 IEEE International Conference on*, 30-35.
- Watanabe, A., Sakakibara, S., Ban, K., Yamada, M., Shen, G. and Arai, T. (2006), "A Kinematic Calibration Method for Industrial Robots Using Autonomous Visual Measurement", *CIRP Annals - Manufacturing Technology*, **55**(1), 1-6. DOI: [http://dx.DOI.org/10.1016/S0007-8506\(07\)60353-9](http://dx.DOI.org/10.1016/S0007-8506(07)60353-9)
- Zimmermann, M., Krishnan, R., Raabe, A. and Seifert, V. (2004), "Robot-assisted navigated endoscopic ventriculostomy: implementation of a new technology and first clinical results", *Acta Neurochirurgica*, **146**(7). Doi: 10.1007/s00701-004-0267-7